

# Monocarboxylate transporters (MCTs) in gliomas: expression and exploitation as therapeutic targets

Vera Miranda-Gonçalves, Mrinalini Honavar, Céline Pinheiro, Olga Martinho, Manuel M. Pires, Célia Pinheiro, Michelle Cordeiro, Gil Bebiano, Paulo Costa, Isabel Palmeirim, Rui M. Reis, and Fátima Baltazar

*Life and Health Sciences Research Institute (ICVS), School of Health Sciences, University of Minho, Campus Gualtar, Braga, Portugal (V.M.-G., C.P., O.M., R.M.R., F.B.); ICVS/3B's-PT Government Associate Laboratory, Braga/Guimarães, Portugal (V.M.-G., C.P., O.M., R.M.R., F.B.); Department of Pathology, Hospital Pedro Hispano, Matosinhos, Portugal (M.H.); Unit of Neuropathology (M.M.P.); Department of Neurosurgery, Centro Hospitalar do Porto, Porto, Portugal (C.P.); Hospital Dr. Nélio Mendonça, Madeira, Portugal (M.C., G.B.); Radiotherapy Service, Centro Hospitalar do Montijo, Barreiro, Setúbal, Portugal (P.C.); Regenerative Medicine Program, Departamento de Ciências Biomédicas e Medicina, Universidade do Algarve, Faro, Portugal (I.P.); and IBB – Institute for Biotechnology and Bioengineering, Centro de Biomedicina Molecular e Estrutural, Universidade do Algarve, Faro, Portugal (I.P.); and Molecular Oncology Research Center, Barretos Cancer Hospital, São Paulo, Brazil (R.M.R.)*

**Background.** Gliomas exhibit high glycolytic rates, and monocarboxylate transporters (MCTs) play a major role in the maintenance of the glycolytic metabolism through the proton-linked transmembrane transport of lactate. However, their role in gliomas is poorly studied. Thus, we aimed to characterize the expression of MCT1, MCT4, and their chaperone CD147 and to assess the therapeutic impact of MCT inhibition in gliomas.

**Methods.** MCTs and CD147 expressions were characterized by immunohistochemistry in nonneoplastic brain and glioma samples. The effect of CHC (MCT inhibitor) and MCT1 silencing was assessed in *in vitro* and *in vivo* glioblastoma models.

**Results.** MCT1, MCT4, and CD147 were overexpressed in the plasma membrane of glioblastomas, compared with diffuse astrocytomas and nonneoplastic brain. CHC decreased glycolytic metabolism, migration, and invasion and induced cell death in U251 cells (more glycolytic) but

only affected proliferation in SW1088 (more oxidative). The effectiveness of CHC in glioma cells appears to be dependent on MCT membrane expression. MCT1 downregulation showed similar effects on different glioma cells, supporting CHC as an MCT1 inhibitor. There was a synergistic effect when combining CHC with temozolomide treatment in U251 cells. In the CAM *in vivo* model, CHC decreased the size of tumors and the number of blood vessels formed.

**Conclusions.** This is the most comprehensive study reporting the expression of MCTs and CD147 in gliomas. The MCT1 inhibitor CHC exhibited anti-tumoral and anti-angiogenic activity in gliomas and, of importance, enhanced the effect of temozolomide. Thus, our results suggest that development of therapeutic approaches targeting MCT1 may be a promising strategy in glioblastoma treatment.

**Keywords:** CD147, CHC, glioblastomas, gliomas, glycolytic metabolism, lactate, monocarboxylate transporters.

Received January 2, 2012; accepted October 17, 2012.

**Corresponding Authors:** Fátima Baltazar, PhD, Life and Health Sciences Research Institute (ICVS), School of Health Sciences, University of Minho, Campus de Gualtar, 4710-057 Braga, Portugal (fbaltazar@ecea.uminho.pt); Rui M. Reis, PhD, Life and Health Sciences Research Institute (ICVS), School of Health Sciences, University of Minho, Campus de Gualtar, 4710-057 Braga, Portugal (rreis@ecea.uminho.pt).

**G**liomas, the most common primary central nervous system (CNS) tumors, have distinct histological subtypes and, according to the latest World Health Organization (WHO) classification, are divided into 4 malignant grades.<sup>1</sup> Glioblastomas

(WHO grade IV) are not only the most frequent, but also the most aggressive CNS tumors. Despite progress in therapy, prognosis of patients with glioblastoma is still very dismal. The current gold standard therapy strategy combines temozolomide with radiotherapy, with an overall survival of only approximately 15 months.<sup>2</sup>

Tumor cells present uncontrolled cell proliferation, and during cancer progression, there are selective active processes, namely adjustments of energy metabolism, to fuel cell growth and division.<sup>3,4</sup> A classical phenomenon that describes this metabolic adaptation is a shift from oxidative phosphorylation to aerobic glycolysis, as a main source of ATP, even in the presence of oxygen, known as the Warburg effect.<sup>5-7</sup> The high rates of glycolytic metabolism produce high levels of lactate/H<sup>+</sup> (lactic acid), and to maintain the enhanced glycolytic flux and intracellular physiological pH, tumor cells perform the efflux of lactic acid into the extracellular microenvironment, preventing intracellular acidosis and consequent cell death.<sup>8</sup> Therefore, tumor cells upregulate pH regulators, such as monocarboxylate transporters (MCTs), among others.<sup>9</sup>

The MCT family comprises 14 members with similar topology; however, only 4 isoforms (MCT1–MCT4) are proton-linked monocarboxylate transporters, performing the transmembrane transport of monocarboxylates, such as lactate, coupled with a proton, in an equimolar manner.<sup>10,11</sup> Monocarboxylate transporters play an important role in mammalian metabolism by regulating distinct pathways.<sup>12,13</sup> In the adult brain, MCT1 is expressed in endothelial cells of microvessels and in astrocytes. MCT2 is expressed in neurons, and MCT4 is present exclusively in astrocytes.<sup>14,15</sup> The difference in MCT isoforms between astrocytes and neurons is explained by the lactate shuttle hypothesis, which states that lactate is produced by astrocytes and used by neurons.<sup>16,17</sup> MCT plasma membrane localization and activity is regulated by coexpression with chaperone proteins,<sup>11,13</sup> namely CD147 (basigin) for MCT1, MCT3, and MCT4 and gp-70 (embigin) for MCT2.<sup>18,19</sup>

Lactate produced by glycolytic tumor cells has an important role in the tumor microenvironment, being associated with poor prognosis.<sup>20</sup> Given the different affinity of the MCT isoforms to lactate,<sup>11</sup> MCT1 and MCT4 are associated with lactate efflux and, therefore, have an important contribution to the maintenance of glycolytic metabolism and consequently tumor cell survival. Several studies described MCT expression in different solid tumors, such as breast,<sup>21</sup> colorectal,<sup>22</sup> cervical,<sup>23</sup> lung,<sup>24</sup> and gastric.<sup>25</sup> However, expression of MCTs in gliomas, in particular, in glioblastomas is not well characterized, and their role is poorly elucidated. There are only a few studies on brain tumors that describe the importance of MCTs in pH homeostasis and tumor growth.<sup>26-30</sup>

Because of the crucial importance of glycolytic metabolism to tumor cells and the pivotal role of MCTs in its maintenance, clarifying the role of MCTs in glioma cell survival, proliferation, and aggressiveness is essential. Thus, our study aimed to explore MCTs as a new therapeutic target in glioblastomas. For that,

assessment of MCT1 and MCT4 expressions, as well as CD147, in a series of human gliomas and evaluation of the clinical-pathological significance of their expression profile was performed. Furthermore, the effect of MCT1 inhibition on the viability, proliferation, survival, and aggressiveness of glioma cells was evaluated in both *in vitro* and *in vivo* models.

## Materials and Methods

### *Tissues Samples*

A series of paraffin-embedded glioma tissue samples was obtained from Hospital Pedro Hispano, Matosinhos, Centro Hospitalar do Porto, Porto, and Hospital do Dr. Nélio Mendonça, Madeira, Portugal. This series was composed of 78 glioblastomas (WHO grade IV), 10 diffuse astrocytomas (WHO grade II), and 24 nontumoral adjacent tissues. The present study was previously approved by Local Ethical Review Committees, and all the samples enrolled in the present study were unlinked and unidentified from their donors.

### *Cell Lines and Cell Culture*

In the present study, 8 high-grade glioma cell lines were used. The cell lines SW1088, SW1783, U87-MG, and A172 were obtained from American Type Culture Collection, the cell lines SNB-19 and GAMG were obtained from German Collection of Microorganisms and Cell Cultures, and the cell lines U251 and U373 were kindly provided by Professor Joseph Costello, California University, Neurosurgery Department, San Francisco. Cell line authentication was performed at IdentiCell Laboratories (Department of Molecular Medicine at Aarhus University Hospital Skejby, Århus, Denmark) in August 2011. Genotyping confirmed the complete identity of all cell lines, except the U373 cell line, which was shown to be a subclone of the U251 cell line. All cell lines were maintained in Dulbecco's Modified Eagle's Medium (DMEM 1×, High Glucose; Gibco, Invitrogen) supplemented with 10% fetal bovine serum (Gibco, Invitrogen) and 1% penicillin-streptomycin solution (Gibco, Invitrogen) at 37°C and 5% CO<sub>2</sub>.

### *Downregulation of MCT1 Expression*

Silencing of MCT1 expression was done with siRNA (siRNA for MCT1, ASO0J7OY, Invitrogen; scramble siRNA, ASO0JDS2, Invitrogen), using lipofectamine (13778-075, Invitrogen) as the permeabilization agent, according to the manufacturer's instructions.

### *Drugs*

Alpha-cyano-4-hydroxycinnamate (CHC; Sigma-Aldrich) and temozolomide (TMZ; Sigma-Aldrich) were dissolved in dimethyl sulfoxide (DMSO; Sigma-Aldrich) to 3 M

and 100 mM stock solutions, respectively, from which the working solutions were prepared.

### Antibodies

For immunohistochemistry, we used the following antibodies and dilutions: MCT1 (1:200 dilution; AB3538P; Chemicon International); MCT4 (1:500 dilution, H-90; sc-50329; Santa Cruz Biotechnology); CD147 (1:500 dilution; 18-7344; Zymed Laboratories Inc), and Ki67 (1:100 dilution; 6599-059; AbD Serotec).

### Immunohistochemistry

Representative 4- $\mu$ m-thick tissue sections were used for immunohistochemical analysis. Immunohistochemistry (IHC) for MCT1 was performed according to the avidin-biotin-peroxidase principle (R.T.U. Vectastin Elite ABC kit; Vector Laboratories), as previously described by our group.<sup>22</sup> For CD147 and MCT4, IHC was performed with the Ultravision Detection System Anti-polyvalent, HRP (Lab Vision Corporation), as previously described.<sup>31</sup> In brief, deparaffinized and rehydrated slides were submitted to heat-induced antigen retrieval for 20 min at 98°C with 10 mM citrate buffer (pH, 6.0) for MCT1 and MCT4 and 1 mM EDTA buffer (pH, 8.0) for CD147. After endogenous peroxidase inactivation, incubation with the primary antibody was performed overnight for MCT1 and 2 h for MCT4 and CD147, at room temperature. The immune reaction was visualized with 3,3'-Diaminobenzidine (DAB+ Substrate System; Dako) as a chromogen. All sections were counterstained with Gill-2 haematoxylin. For negative controls, primary antibodies were omitted and also replaced by a universal negative control antibody (N1699, Dako). Colon carcinoma tissue was used as positive control for MCT1, MCT4, and CD147. Tissue immunostaining was evaluated semiquantitatively, considering extension and intensity of staining, as published previously.<sup>22</sup> The score for immunoreactive extension was as follows: score 0, 0% of immunoreactive cells; score 1, <5% of immunoreactive cells; score 2, 5%–50% immunoreactive cells; and score 3, >50% of immunoreactive cells. For intensity, the score was as follows: 0, negative; 1, weak; 2, intermediate; and 3, strong. The final score was defined as the sum of these 2 semiquantitative scores, and for statistical analysis, final score >3 was considered to be positive. Cellular localization of staining (cytoplasm/membrane) of the studied markers was also evaluated.

### Immunocytochemistry

Paraffin cytoblocks were made from concentrated cell suspensions by centrifuging fresh cell suspensions at 1200 rpm for 5 min. Cell pellets were incubated with formaldehyde 3.7% overnight and recentrifuged. Cell pellets were then processed in an automatic tissue processor (TP1020; Leica), before inclusion into paraffin (block-forming unit EG1140H; Leica). Immunocytochemistry

for MCT1, MCT4, and CD147 was performed in 4  $\mu$ m cytoblock sections, according to the protocol mentioned for paraffin tissues. Cells were evaluated for protein expression, distinguishing cytoplasmic from membrane expression.

### Western Blotting

Parental glioma cell lines and siMCT1 cells were grown to 80% confluence, homogenized in lysis buffer (supplemented with protease inhibitors) for 15 min, and then centrifuged at 13 000 rpm for 15 min at 4°C. The supernatants were collected, and protein quantification was performed according to the Bio-Rad Dc Protein Assay (500-0113, Bio Rad). Aliquots of 20  $\mu$ g of total protein were separated on 10% polyacrylamide gel by SDS-PAGE and transferred onto a nitrocellulose membrane (Amersham Biosciences) in 25 mM Tris-base/glycine buffer. Membranes were blocked with 5% milk in TBS/0.1% Tween (TBS-T; pH = 7.6) for 1 h at room temperature. After incubation overnight at 4°C with the primary polyclonal antibodies for MCT1 (1:200 dilution; AB3538P; Chemicon International), MCT4 (1:500 dilution, H-90; sc-50329; Santa Cruz Biotechnology), and CD147 (1:500 dilution; 18-7344; Zymed Laboratories), membranes were washed in TBS/0.1% Tween and incubated with the secondary antibody coupled to horseradish peroxidase (SantaCruz Biotechnology). The bound antibodies were visualized by chemiluminescence (Supersignal West Femto kit; Pierce), and quantification of Western blot results using band densitometry analysis was performed with the Image J software (version 1.41; National Institutes of Health).  $\beta$ -Actin was used as loading control at 1:300 dilution (I19, sc-1616; Santa Cruz Biotechnology).

### Cell Viability and Proliferation Assays

Cells were plated into 96-well plates, at a density of  $3 \times 10^3$  cells per well. The effect of treatment with CHC (0.6–12 mM) on cell number (total biomass) was determined at 24, 48, and 72 h by the sulforhodamine B assay (SRB, TOX-6; Sigma-Aldrich), according to the manufacturer's recommendations. IC<sub>50</sub> values (i.e., CHC concentration that corresponds to 50% of cell growth inhibition) were estimated from 3 independent experiments, each one in triplicate, using GraphPad Software. Cell proliferation assay was performed as previously described<sup>32</sup> and assessed under the treatment conditions previously described, for 5 mM and 10 mM of CHC. After CHC treatment, cells were incubated with BrdU and its incorporation was assessed at 450 nm ( $\lambda_{\text{ref}} = 655$  nm), according to the manufacturer's protocol (BrdU, Cell Proliferation ELISA; Roche Diagnostics). Cell growth (total biomass) and cell proliferation for glioma siMCT1 cells and the effect of CHC (1.25–15 mM) on cell number were performed as described above.

### Drug Combination Studies

A density of  $3 \times 10^3$  U251 cells/well were seeded into 96-well plates. Treatments with TMZ (0.01–1 mM), CHC (0.6–12 mM), and TMZ + CHC (0.05–0.5 mM TMZ + 5 mM CHC) were done for 72 h. The effect of TMZ and CHC alone or in combination on cell growth was evaluated using the SRB assay, as described above. The combined effect of the drugs was determined using the CalcuSyn Software (Biosoft). Synergy or antagonism was quantified by the combination index (CI), where  $CI = 1$  indicates an additive effect,  $CI < 1$  indicates synergy, and  $CI > 1$  indicates antagonism.<sup>33</sup>

### Metabolism Assay (Extracellular Glucose and Lactate Measurements)

Cells were plated in 48-well plates at a density of  $4 \times 10^4$  cells per well and allowed to adhere overnight. Then, cells were treated with 5 mM and 10 mM CHC, and the cell culture medium was collected after 8, 12, and 24 h for glucose and lactate quantification. For these time points, the total protein (expressed as total biomass) was assessed using the SRB assay. Cellular metabolism for glioma siMCT1 cells was assessed for 12 and 24 h. Glucose and lactate were quantified using commercial kits (Roche and Spinreact, respectively), according to the manufacturer's protocols. Results are expressed as total  $\mu\text{g}$ /total biomass.

### Apoptosis Assay

Apoptotic and necrotic cell populations were determined by Annexin V-FLOUS Apoptosis Kit (Roche Diagnostics) according to the manufacturer's instructions. For that,  $2.5 \times 10^5$  cells/well were seeded into 6-well plates in DMEM culture medium. Cells were treated with the  $IC_{50}$  value of CHC for 72 h. After that, cells were collected and Annexin V/PI staining was performed according to the manufacturer's instructions and incubated for 15 min at room temperature. The percentage of cell death was assessed by flow cytometry (LSRII model, BD Biosciences), a total of 50 000 events, and the results were analyzed using the FlowJo software (version 7.6; Tree Star).

### Wound-Healing Assay

Cells were seeded in 6-well plates and cultured to at least 95% of confluence, and wound-healing assay was performed as described previously.<sup>32,34</sup> Cells were treated with 5 and 10 mM CHC for 24 h, and the wound areas were photographed at 0 and 24 h. The relative migration distances were analyzed using Image J Software (version 1.41; National Institutes of Health). The relative migration for siMCT1 glioma cells was assessed as described above.

### Invasion Assay

Cell invasion in U251 and SW1088 cells was performed using 24-well BD Biocoat Matrigel Invasion Chambers, according to the manufacturer's instructions (354480, BD Biosciences). In brief, after matrigel invasion chamber rehydration, cells were seeded and incubated with 5 mM and/or 10 mM CHC for 24 h. Then, non-invading cells were removed and invading cells were fixed with methanol and stained with hematoxylin. Membranes were photographed in Olympus SZx16 stereomicroscope (16 $\times$ ), and invading cells were counted using the Image J software (version 1.41; National Institutes of Health). Invasion was calculated as percentage of cell invasion normalized for the control condition.

### Chicken Chorioallantoic Membrane (CAM) Assay

CAM assay was performed as previously described.<sup>32,34</sup> In brief, fertilized chicken eggs (Pinto Bar) were incubated at 37°C. On day 3 of development, a window was made into the eggshell after puncturing the air chamber, and eggs were sealed with BTK tape and returned to the incubator. On day 9 of development, a ring was placed on the CAM, and on day 10, the U251 cell line ( $2 \times 10^6$  cells in 20  $\mu\text{L}$  DMEM medium) was placed inside the ring and the eggs were tapped and returned to the incubator. At day 14 of incubation, the control group received 40  $\mu\text{L}$  of 1% DMSO in DMEM without fetal bovine serum and the treated group received 40  $\mu\text{L}$  of 5 mM CHC. After 72 h (day 17 of development), the chicken embryos were sacrificed by placing them at  $-80^\circ\text{C}$  for 10 min. CAMs with tumors were dissected, fixed in 4% paraformaldehyde at room temperature, and included in paraffin. Immunohistochemistry on paraffin sections of microtumors was performed for MCTs, as previously described for the human samples. The effect of CHC on cell proliferation was assessed by Ki67 immunohistochemistry using the avidin-biotin-peroxidase method (R.T.U. Vectastin Elite ABC kit, Vector Laboratories). Antigen retrieval was performed in the microwave with 10 mM citrate buffer (pH = 6) for 15 min. Digital Images were taken on days 14 and 17 of development in a stereomicroscope (Olympus S2  $\times$  16), using a digital camera (Olympus DP71). At the selected time points, the in ovo tumor perimeter was measured using the Cell B software (Olympus). Before paraffin inclusion, tumors were photographed ex ovo for blood vessel count. The number of blood vessels was counted in the area inside the ring placed previously in the CAM, using Image J software (version 1.41; National Institute of Health). CHC effect on CAM vascularization was performed at day 14 of development for 72 h. At day 17, the CAM was photographed ex ovo for blood vessel count, as described above.

### Statistical Analysis

Data from human tissue samples were analyzed using SPSS statistical software (version 18.0; SPSS).

The comparison of MCTs and CD147 expressions among nontumoral, diffuse astrocytomas, and glioblastoma tissues was evaluated for statistical significance using the Pearson's  $\chi^2$  test, with the threshold for significance being  $P \leq .05$ . Analyses of associations between MCTs and CD147 expressions in glioblastomas and associations with clinical-pathological data were performed using the same statistical analysis. For the *in vitro* studies, the GraphPad prism 5 software was used, with the Student's *t*-test, considering significant values to be  $P \leq .05$ .

## Results

### Expression of MCT1, MCT4, and CD147 in Human Brain Samples

In the present study, 24 nonneoplastic adjacent brain tissues, 10 diffuse astrocytoma (WHO grade II), and 78 glioblastoma (WHO grade IV) tissues were characterized for MCT1, MCT4, and CD147 immunohistochemical expression (Table 1). MCT1, MCT4 and CD147 were expressed in few cases of nonneoplastic brain tissues (29.2% [7/24], 10.0% [2/20], and 4.6% [1/22], respectively). In diffuse astrocytomas, MCT1 and MCT4 were both expressed in 80.0% (8/10) of cases, and CD147 was expressed in 40.0% (4/10). MCT1, MCT4, and CD147 were highly expressed in glioblastomas (87.2% [68/78], 91.0% [71/78], and 77.9% [60/77], respectively) (Table 1). There was a significant increase in MCT1, MCT4, and CD147 expressions in glioblastomas, compared to nontumoral tissues. In addition, CD147 expression increased significantly from diffuse astrocytomas to glioblastomas, but not MCT1 or MCT4 expressions (Table 1). Of note, MCT1, MCT4, and CD147 were present only in the cytoplasm in nontumoral brain tissue and diffuse astrocytomas (Table 1, Fig. 1). On the other hand, MCT1 and CD147 were expressed in the plasma membrane of almost all positive

glioblastoma cases, whereas MCT4 was only expressed in 56.3% of the total glioblastomas (Table 1, Fig. 1). With regard to positivity for plasma membrane expression, significant associations between MCT1 and CD147 (72.3% [44/61];  $P < .001$ ) and between MCT4 and CD147 (77.5% [31/40];  $P < .001$ ) were observed. No significant associations were found between MCT1, MCT4, and CD147 expressions and clinical-pathological data, such as age, sex, recurrence, and death ( $P > .05$ ; Table 2). In addition, no correlation between MCT1, MCT4, and CD147 expressions with overall survival was observed using a Kaplan–Meier analysis ( $P = .101$ ,  $P = .850$ ,  $P = .871$ , respectively; data not shown). Furthermore, both MCT1 and CD147 were expressed in microvessels and capillaries of nonneoplastic brain tissue and diffuse astrocytomas (Fig. 1).

### Expression of MCT1, MCT4, and CD147 in Glioma Cell Lines

All glioma cell lines expressed MCT1 and MCT4 and CD147, however, with distinct levels, as detected by Western blot and immunocytochemistry (Fig. 2). There was prominent MCT1 expression at the plasma membrane of U251, U373, SNB-19, and GAMG cells. MCT4 was expressed at the plasma membrane in U251, U373, SW1783, and GAMG cell lines, whereas for SW1088 and U87 cells, expression was only present in the cytoplasm. CD147 was expressed at the plasma membrane in almost all cell lines.

### In Vitro Effect of CHC on Glioma Cells

To assess the role of MCTs on glioblastoma behavior, we used the classical MCT inhibitor CHC. There is evidence that CHC inhibits MCT1 activity, with no apparent cytotoxicity *in vivo*.<sup>35,36</sup> First, we started to measure the effect of CHC on cell viability. The response of

**Table 1.** Monocarboxylate transporters (MCT1 and MCT4) and CD147 expressions in nontumoral and glioma tissues

Isoform	n	Immunoreaction			Plasma Membrane		
		Positive	%	P*	Positive	%	P*
<b>MCT1</b>							
Nontumoral	24	7	29.2	<.001	0	0.0	<.001
Diffuse astrocytoma	10	8	80.0	.621	0	0.0	<.001
Glioblastoma	78	68	87.2		61	78.2	
<b>MCT4</b>							
Nontumoral	20	2	10.0	<.001	0	0.0	.001
Diffuse astrocytoma	10	8	80.0	.224	0	0.0	<.001
Glioblastoma	78	71	91.0		40	56.3	
<b>CD147</b>							
Nontumoral	22	1	4.6	<.001	0	0.0	<.001
Diffuse astrocytoma	10	4	40.0	.019	0	0.0	<.001
Glioblastoma	77	60	77.9		56	72.7	

\*Association with glioblastoma tissue.

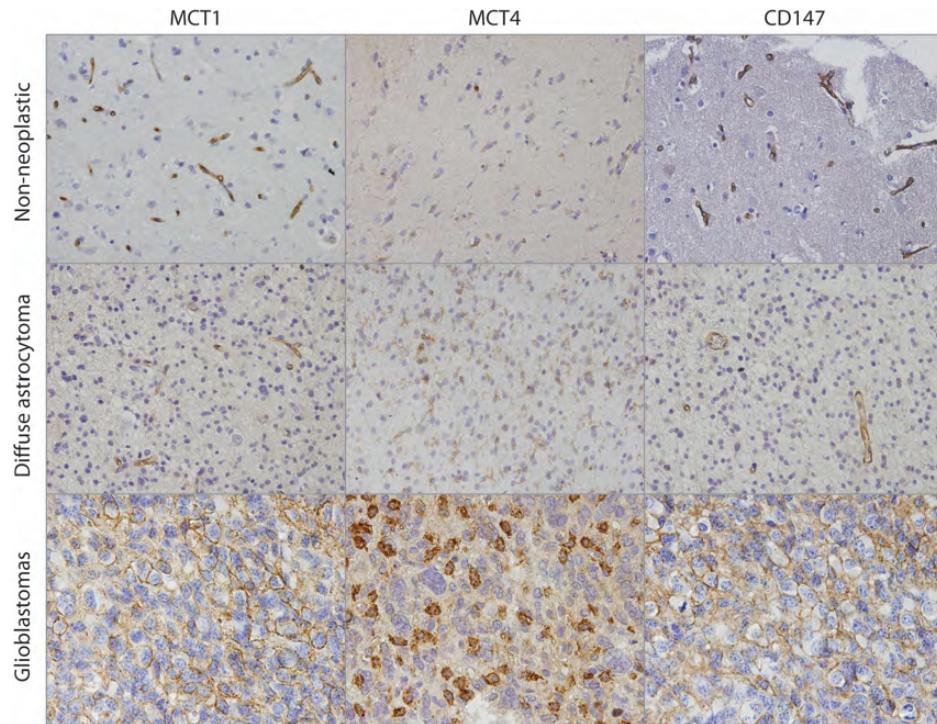


Fig. 1. Immunohistochemical expression of monocarboxylate transporters and their chaperone protein CD147 in glioma samples. MCT1 and MCT4 isoforms and their chaperone CD147 presented weak cytoplasmic expression in few cases of nontumoral cerebral tissue. Diffuse astrocytomas presented cytoplasmic expression of MCT1, MCT4, and CD147. Glioblastoma tissues present a strong expression of MCT1 and CD147, mainly at the plasma membrane, whereas MCT4 reactivity was found in both the cytoplasm and the plasma membrane. Pictures were obtained using the microscope Olympus BX61, at 400 $\times$  magnification.

**Table 2.** Associations of monocarboxylate transporters (MCT1 and MCT4) and CD147 expressions with clinical-pathological features

Feature	n	MCT1		n	MCT4		n	CD147	
		Positive (%)	P		Positive (%)	P		Positive(%)	P
Death	59	37 (62.7)	.671	59	41 (69.5)	.564	58	34 (58.6)	.727
Recurrence	58	25 (43.1)	.167	58	31 (53.4)	.316	57	24 (42.1)	.484
Age			.731			.678			.216
$\geq 55$ years	76	37 (48.7)		76	41 (53.9)		75	36 (48.0)	
$< 55$ years		29 (38.2)			28 (37.3)			23 (30.7)	
Sex			.505			.446			.377
Male	75	38 (50.7)		75	42 (56.0)		74	34 (45.9)	
Female		27 (36.0)			27 (36.0)			25 (33.8)	

glioma cell lines to CHC ( $IC_{50}$  values) was estimated after 72 h of treatment (see Supplementary material, Fig. S1 and Table S1). We found that, in the range of 0.6–12 mM of CHC, glioma cells present a decrease in total biomass (SRB assay). Most cell lines presented  $IC_{50}$  values for CHC of 2.5–5.1 mM CHC, with higher values for SW1088 and SW1783 cell lines (10.8 mM and 7.1 mM CHC, respectively) (see Supplementary material, Table S1). For subsequent studies, 2 cell lines were chosen on the basis of their opposite response to CHC: U251, one of the most sensitive cells, and SW1088, the least-sensitive cell line (see Supplementary material, Table S1). CHC decreased the total cell biomass over time in a dose-dependent

manner in U251 cells; however, the CHC effect was smaller on SW1088 cells (Fig. 3A). We assessed the glycolytic rates of both cell lines by measuring the extracellular levels of glucose and lactate over time. As can be seen in Fig. 3B, U251 exhibited higher glycolytic rates than SW1088 cells. Then, to evaluate the effect of CHC on metabolic disturbance, glucose consumption and lactate production were evaluated for 8, 12, and 24 h, using 5 mM and 10 mM CHC for U251 and SW1088 cells. Results for U251 showed a significant decrease in glucose consumption for 12 and 24 h and in lactate production for 12 h for 10 mM CHC and 24 h for both 5 mM and 10 mM CHC, compared with untreated cells (Fig. 3C). For SW1088, only 10 mM

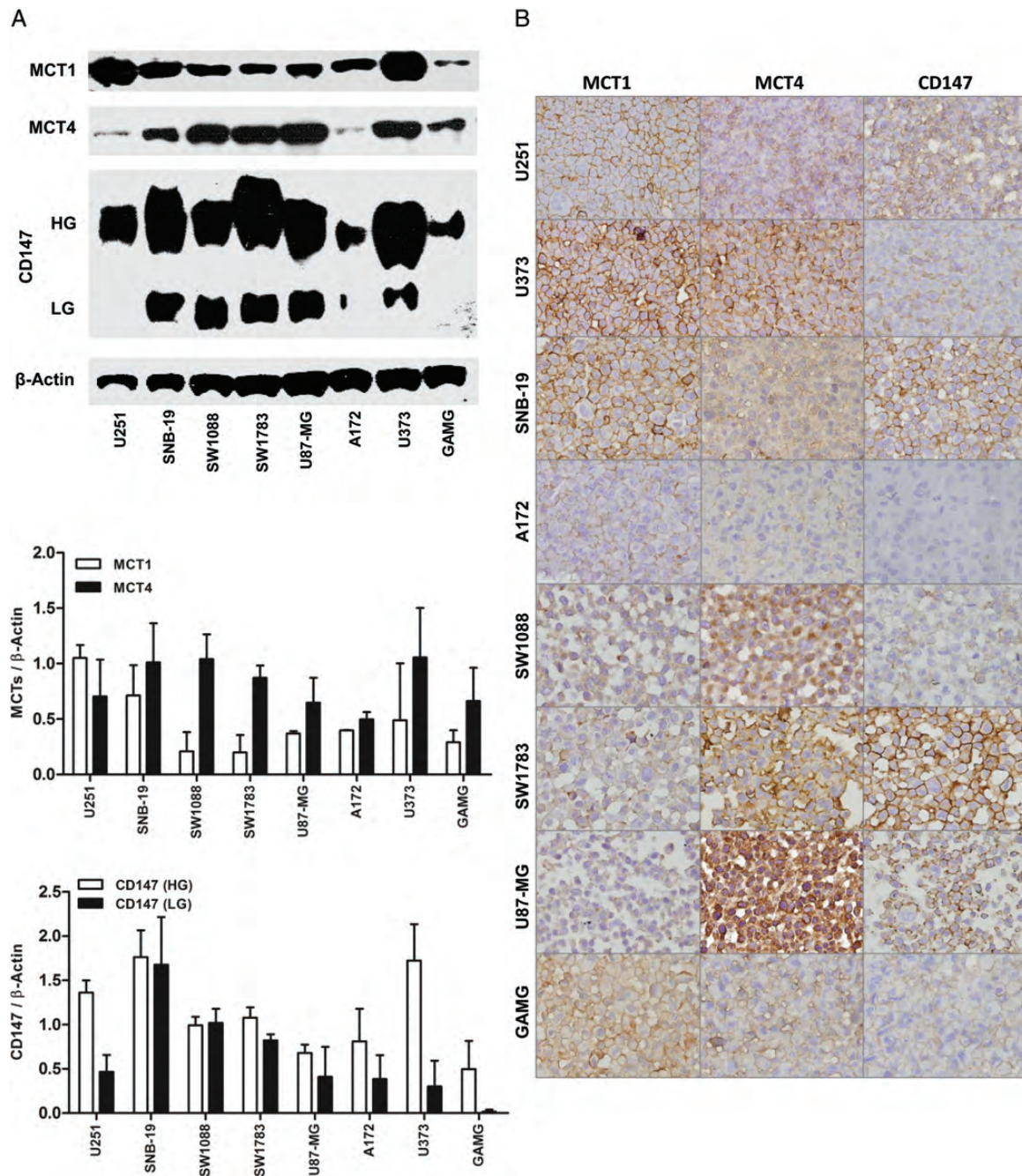


Fig. 2. Monocarboxylate transporters (MCT1 and MCT4) and CD147 expressions in glioblastoma cell lines. (A) Western blot analysis of MCT1, MCT4, and CD147 showing different levels of expression in glioma cells. The molecular weights (kDa) are the following: 50 kDa for MCT1, 52 kDa for MCT4, and 50–60 kDa for the highly glycosylated and 42 kDa for low glycosylated form of CD147. Results are presented as the mean  $\pm$  SD of 2 independent cell lysates. (B) Immunocytochemistry analysis of MCT1, MCT4, and CD147 expressions in glioma cells (400 $\times$  magnification). MCT1 is mainly expressed at the plasma membrane of U251, U373, SNB-19, and GAMG glioma cell lines, whereas MCT4 is present at both plasma membrane and cytoplasm of the different glioma cells. CD147 is expressed at the plasma membrane of some glioma cells, with different levels.

CHC produced a significant decrease in glucose consumption for 24 h, with no significant effect on lactate production over time (Fig. 3C).

In cell proliferation analysis assessed by BrdU assay, CHC decreased the proliferation of U251 over time for

the 2 CHC concentrations used (5 mM and 10 mM), whereas for SW1088, this effect was only seen for 10 mM CHC at 72 h of treatment (Fig. 4A). To determine the effect of CHC on glioma cell death and cell cycle distribution, U251 and SW1088 cells were

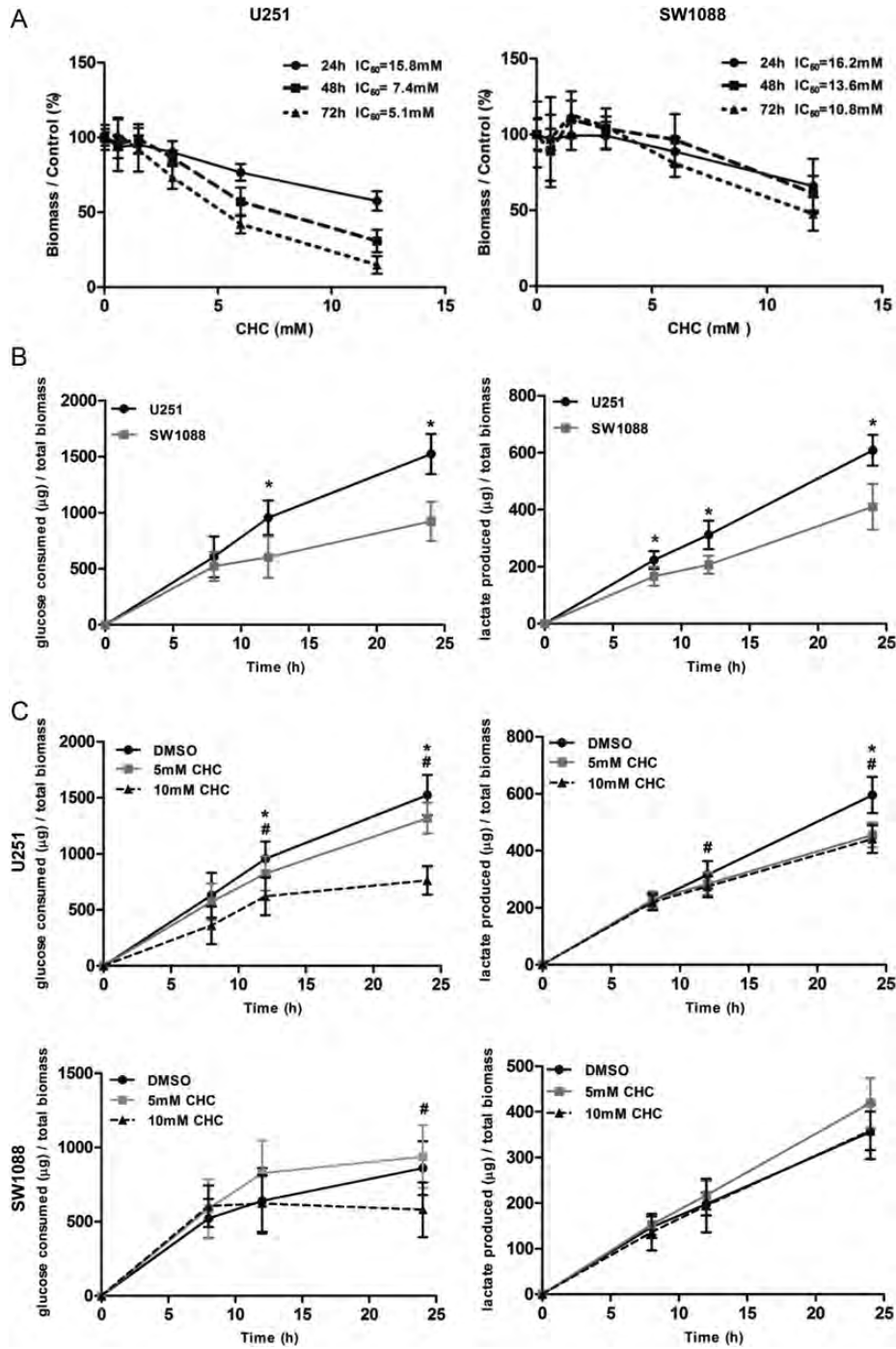


Fig. 3. Effect of the MCT inhibitor, CHC, on total cell biomass and cellular metabolism. (A) The effect of CHC on total biomass of glioma cells was evaluated over time by the sulphorhodamine B assay. CHC inhibited the viability of U251 cells, but not SW1088, over time, in a dose-dependent manner. (B) Metabolic characterization of U251 and SW1088 cells. U251 cells presented higher levels of glucose consumption and lactate production than SW1088 cells. \* $P \leq .05$ , compared U251 with SW1088 cells. (C) The effect of CHC on cellular metabolism was evaluated by extracellular glucose and lactate measurements. CHC induced a significant decrease in glucose consumption and lactate production on U251, compared with SW1088 cells. Results were normalized to total biomass, at each time point. \* $P \leq .05$ , compared 5 mM CHC with DMSO. # $P \leq .05$ , compared 10 mM CHC with DMSO. Results are expressed as the mean  $\pm$  SD of at least 3 independent experiments, each in triplicate.

treated during 72 h with 5 mM and 10 mM CHC, respectively. U251 presented a significant increase in the cell population of subG0 phase and a decrease in the

cell population of G0/G1 phase of the cell cycle, compared with the control. However, in SW1088, there was a significant increase in the cell population of S



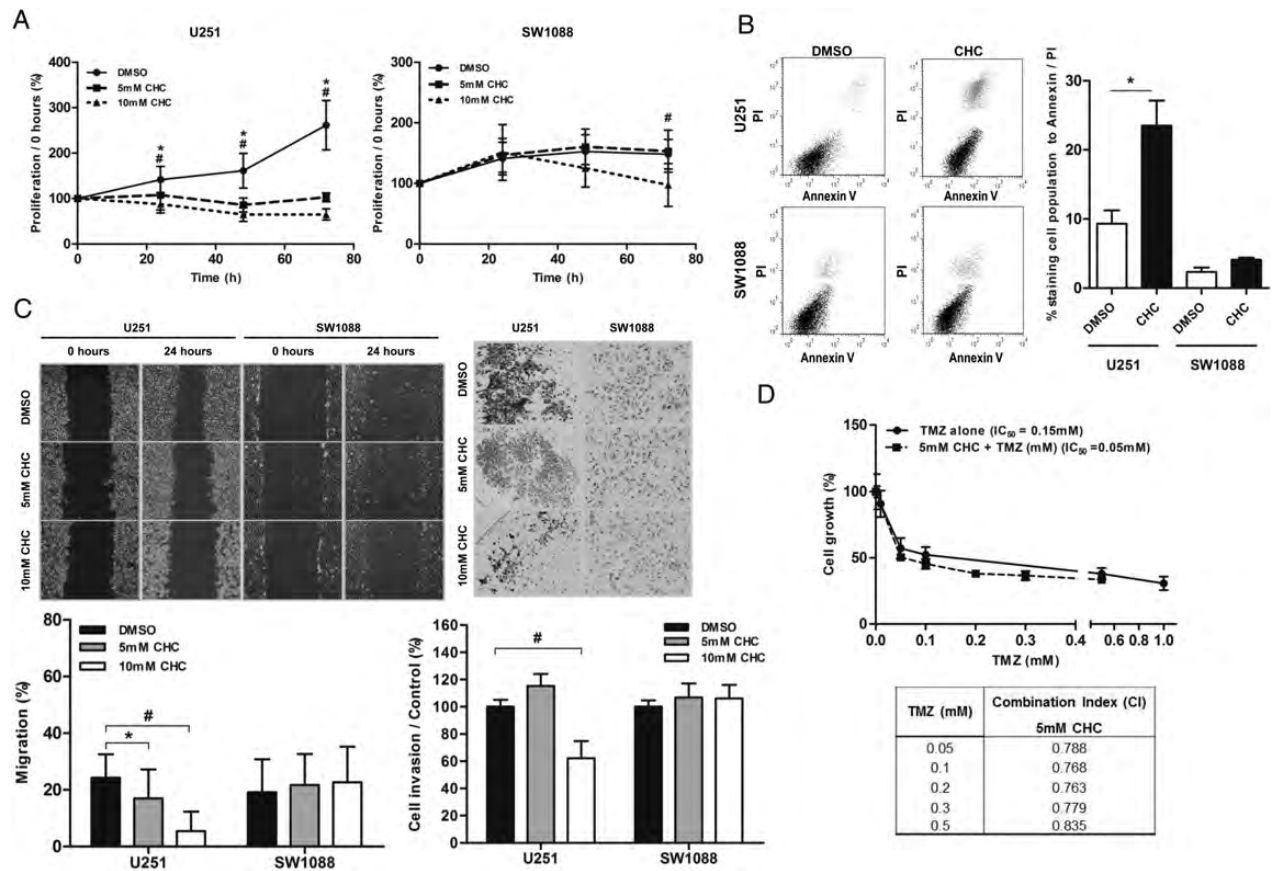


Fig. 4. Effect of CHC on glioma cell behavior and response to TMZ. (A) The effect of CHC on cell proliferation was determined using the BrdU assay. CHC had a significant effect on the cellular proliferative capacity of U251 cells over time, and for SW1088, CHC only had an effect for 10 mM CHC at 72 h. \* $P \leq .05$ , compared 5 mM CHC with DMSO. # $P \leq .05$ , compared 10 mM CHC with DMSO. Results are expressed as the mean  $\pm$  SD of at least 3 independent experiments, each in triplicate. (B) Cell death analysis was done in U251 and SW1088 cells after 72 h of treatment with  $IC_{50}$  values of CHC by Annexin V/PI assay (flow cytometry). In U251 cells, we observed a significant increase in cell death induced by CHC, whereas for SW1088, there was no difference (right panel). Representative dotplot of cell population distribution stained for Annexin V and PI are shown in the left panel (cell population in bottom/left = viable cells; the cell population in upper/right = death cells [late apoptosis/necrosis]). \* $P \leq .05$ . Results are expressed as the mean  $\pm$  SD of at least 3 independent experiments; (C) In the wound-healing migration assay and matrigel invasion assay, we observed that CHC decreased U251 cell migration, compared with control cells, but not for SW1088 cells. Representative images of the migration assay at 0 and 24 h are presented (40 $\times$  magnification) (left panel). For invasion assay, representative images at 24 h are shown (100 $\times$  magnification) (right panel); \* $P \leq .05$ , compared 5 mM CHC with DMSO. # $P \leq .05$ , compared 10 mM CHC with DMSO. Results are expressed as the mean  $\pm$  SD of at least 3 independent experiments. (D) Effect of CHC + TMZ treatment in U251 cell growth was evaluated by SRB at 72 h. U251 cells were treated with fixed concentration of CHC (5 mM) and increasing concentrations of TMZ (0.05–0.5 mM). TMZ + CHC therapy decreased cell growth of U251 cells, compared with TMZ alone (graph). Growth curves for TMZ and CHC in monotherapy were compared with the combination to determine the combination index (CI) for each concentration of TMZ (table). Values  $< 1$  indicate a synergistic drug relationship; results are representative of 3 independent experiments, each in triplicate.

phase with a decrease in the cell population of G0/G1 phases, but without effect in the cell population of subG0 phase (see Supplementary material, Fig. S2). Through the Annexin V/PI assay, we observed that CHC induced cell death in U251 cells, but not in SW1088, by a significant increase in late apoptotic/necrotic cell population (Fig. 4B). According to these results, CHC induced cell death in the U251 cell line, having only an effect on proliferation of SW1088 cells. Thus, CHC appears to have a cytotoxic effect in U251 cells and a cytostatic effect in SW1088 cells.

The importance of MCT activity on cellular migration and invasion capacity was assessed by the wound-healing assay and matrigel invasion assay, respectively. Treatment with CHC decreased U251 cell migration for both concentrations of CHC (5 mM and 10 mM), but not for SW1088 cells (Fig. 4C). In addition, we observed that 10 mM of CHC induced a significant decrease in U251 cell invasion (Fig. 4C).

To evaluate the effect of the combination of CHC and TMZ, we assessed U251 cell total biomass with use of the SRB assay. CHC potentiated the effect of TMZ,

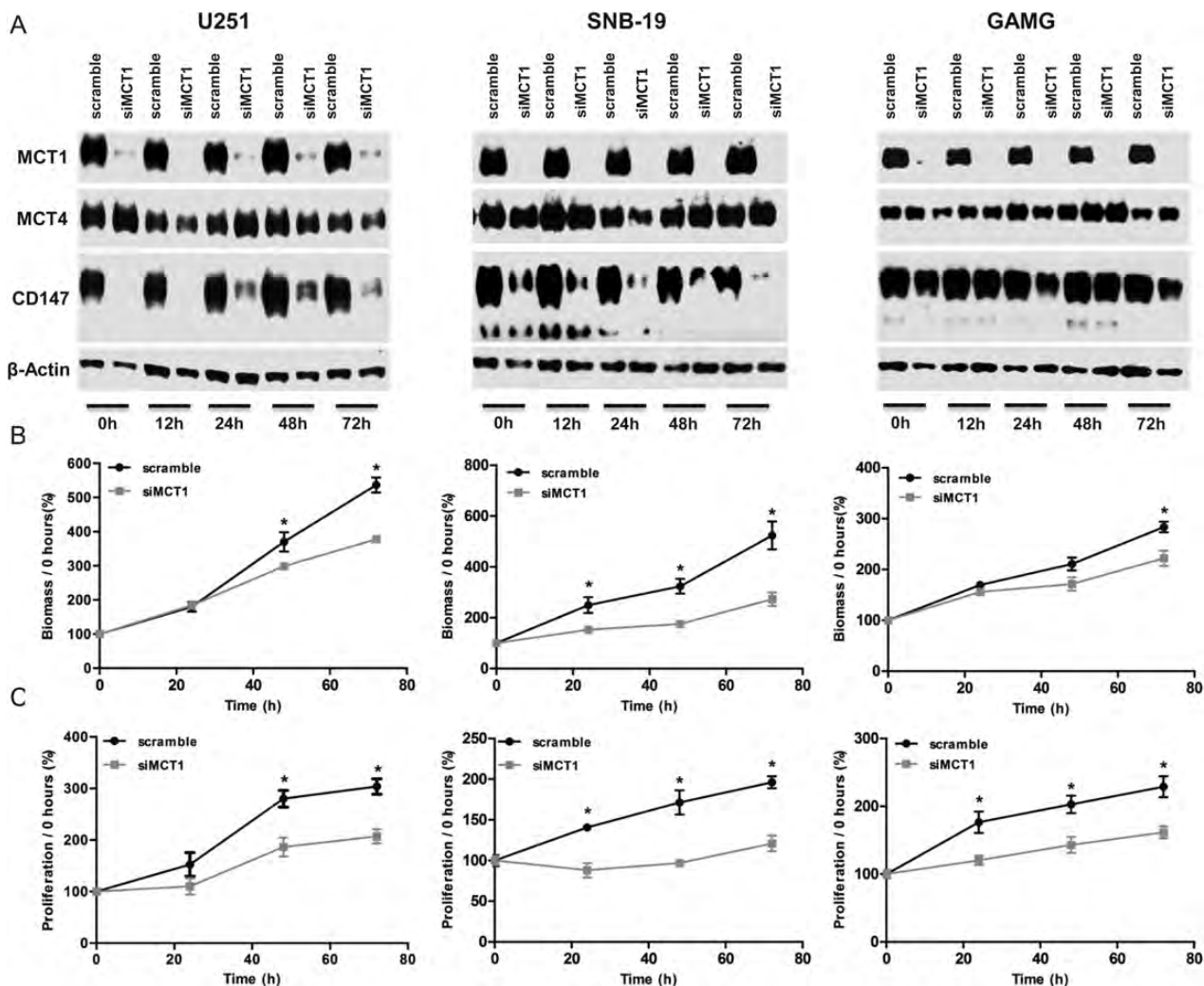


Fig. 5. Effect of MCT1 downregulation on cell growth and proliferation. (A) Western blot analysis of MCT1, MCT4, and CD147 expressions in siMCT1 U251, SNB-19, and GAMG cells. Molecular weights (kDa) are the following: 50 kDa for MCT1, 52 kDa for MCT4, and 50–60 kDa for the highly glycosylated and 42 kDa for the low glycosylated form of CD147. (B) Cell growth and (C) cell proliferation decreased with MCT1 downregulation. \* $P \leq .05$ , siMCT1 cells compared with scramble. Results represent the mean  $\pm$  SD of at least 3 independent experiments, each in triplicate.

decreasing its  $IC_{50}$  value (Fig. 4D). The CI was  $<1$  (Fig. 4D), confirming the synergistic effect of the combination of CHC with TMZ.

To further confirm CHC inhibition of MCT1 as the mechanism of selective toxicity observed in glioblastoma cells, we performed downregulation of MCT1 with use of siRNA in U251, SNB-19, and GAMG cell lines, which exhibited MCT1 expression at the plasma membrane. Downregulation of MCT1 in all 3 cell lines led to an efficient decrease in MCT1 expression, which was accompanied by decrease of CD147 expression in U251 and SNB-19 cells (Fig. 5A). No effect on MCT4 expression was observed in all 3 cell lines (Fig. 5A). Similar to MCT1 activity inhibition, downregulation of MCT1 in glioma cells led to a decrease in cell growth over time, being only significant for GAMG cells for 72 h (Fig. 5B). Likewise, cell proliferation decreased over time for the 3 cell lines (Fig. 5C).

Downregulation of MCT1 also induced a significant decrease in lactate production in U251 and SNB-19 cells for 12 and 24 h and in GAMG cells for 24 h (Fig. 6A), supporting the role of MCT1 in the maintenance of glycolytic rates. In addition, it was observed that downregulation of MCT1 induced a significant decrease in the cellular migration of U251, SNB-19, and GAMG cells (Fig. 6B). Downregulation of MCT1 increased the  $IC_{50}$  values for CHC, compared with control cells, up to 72 h (Fig. 7A) in all glioma cells used. Furthermore, treatment of siMCT1 cells with CHC did not alter lactate production (Fig. 7B).

#### *In Vivo Effect of CHC on Glioma Cells*

U251 cell line exhibits higher glycolytic rates, and according to the in vitro results obtained in this study, MCT activity appears to have an important role on

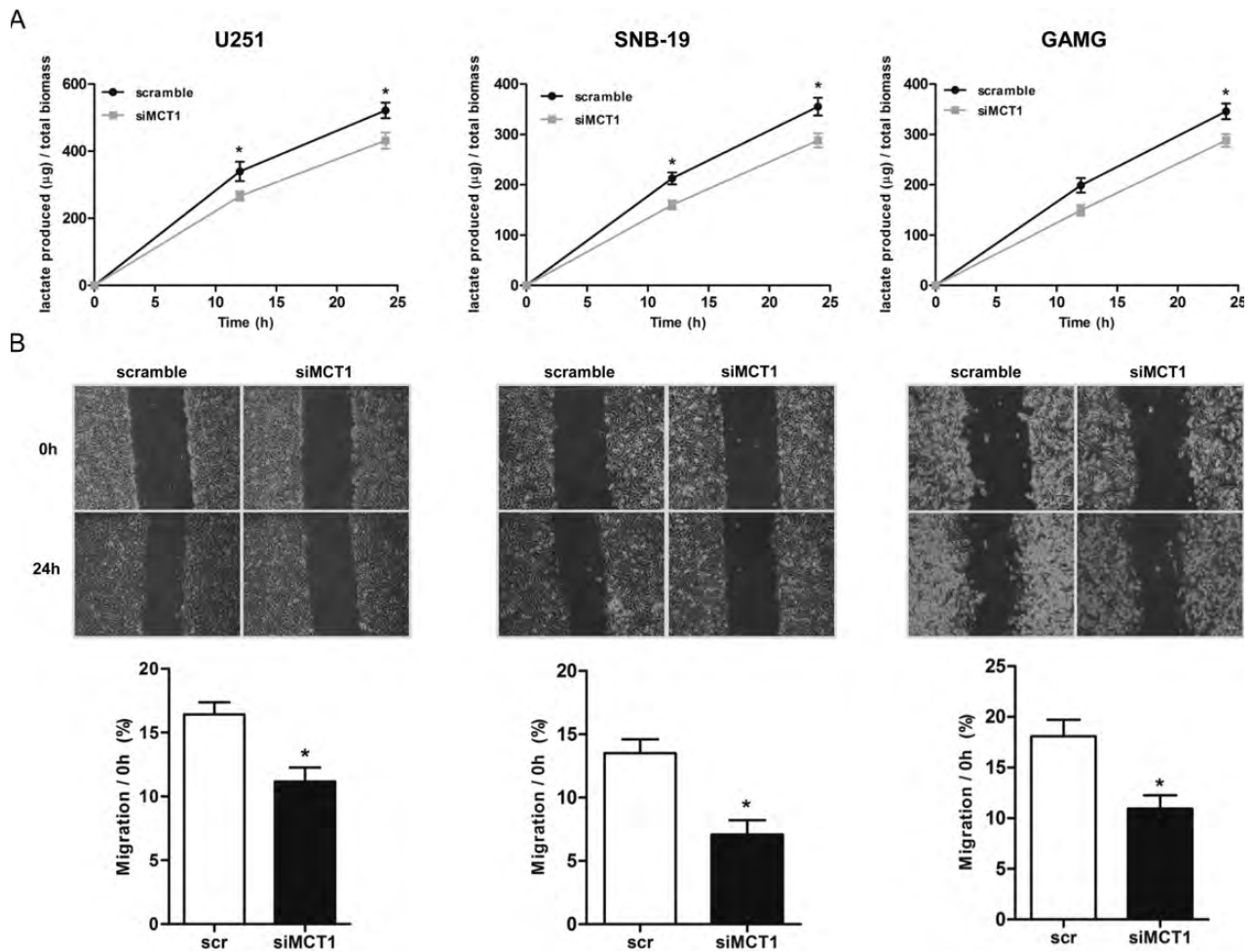


Fig. 6. Effect of MCT1 downregulation on lactate production and cell migration. (A) Lactate production decreased at 12 and 24 h in both siMCT1 U251 and SNB-19 cells and only at 24 h in GAMG cells. Results represent the mean  $\pm$  SD of at least 3 independent experiments, each in triplicate. \* $P \leq .05$ , siMCT1 cells compared with scramble. (B) Downregulation of MCT1 decreased the migration capacity of cells by the wound-healing assay. Results represent the mean  $\pm$  SD of at least 3 independent experiments. \* $P \leq .05$ , siMCT1 cells compared with scramble.

cell growth, migration, and invasive capacity of these cells. Thus, we evaluated the potential of CHC *in vivo* with use of the chicken CAM assay,<sup>37</sup> which allows a 3D tumor formation that is important in the context of tumor microenvironment and cellular metabolism. U251 cells were grown in the CAM of chicken embryos for 4 days, and treatment with 5 mM CHC was initiated. As shown in Fig. 8A, we observed a difference in tumor size between the control and treated group and in the number of blood vessels formed around the tumor. CHC induced a significant decrease in the perimeter of the tumors of the treated group (3.6 mm), compared with the control group (5.2 mm), after 72 h (Fig. 8B). This treatment also induced a significant decrease in the number of blood vessels around the tumors in the treated group (45 vessels), compared with the control group (35 vessels) (Fig. 8B). In addition, CHC decreased the proliferation of tumors, presenting 25% Ki67 positive cells in the control group ( $n = 5$ ), compared with 5% in the CHC group ( $n = 5$ ) (Fig. 8C

and D). However, there was no clear difference in MCT1 and MCT4 expressions between the control and CHC group (Fig. 8C), corroborating the results obtained *in vitro* (see Supplementary material, Fig. S3).

Furthermore, CHC did not decrease the number of blood vessels when put alone in the CAM under the same conditions (Supplementary material, Fig. S4), demonstrating that CHC effect is mediated by the tumor cells and not directly on the CAM vessels.

## Discussion

Glioblastomas are very aggressive human neoplasms, presenting high resistance to current therapy.<sup>2</sup> Thus, exploitation of new molecular targets becomes crucial in neuro-oncology. It is well established that solid tumors, including glioblastomas, present hypoxic regions and increased glycolysis. It is described that glycolysis is upregulated >3-fold in glioblastomas that in normal brain,<sup>38</sup>

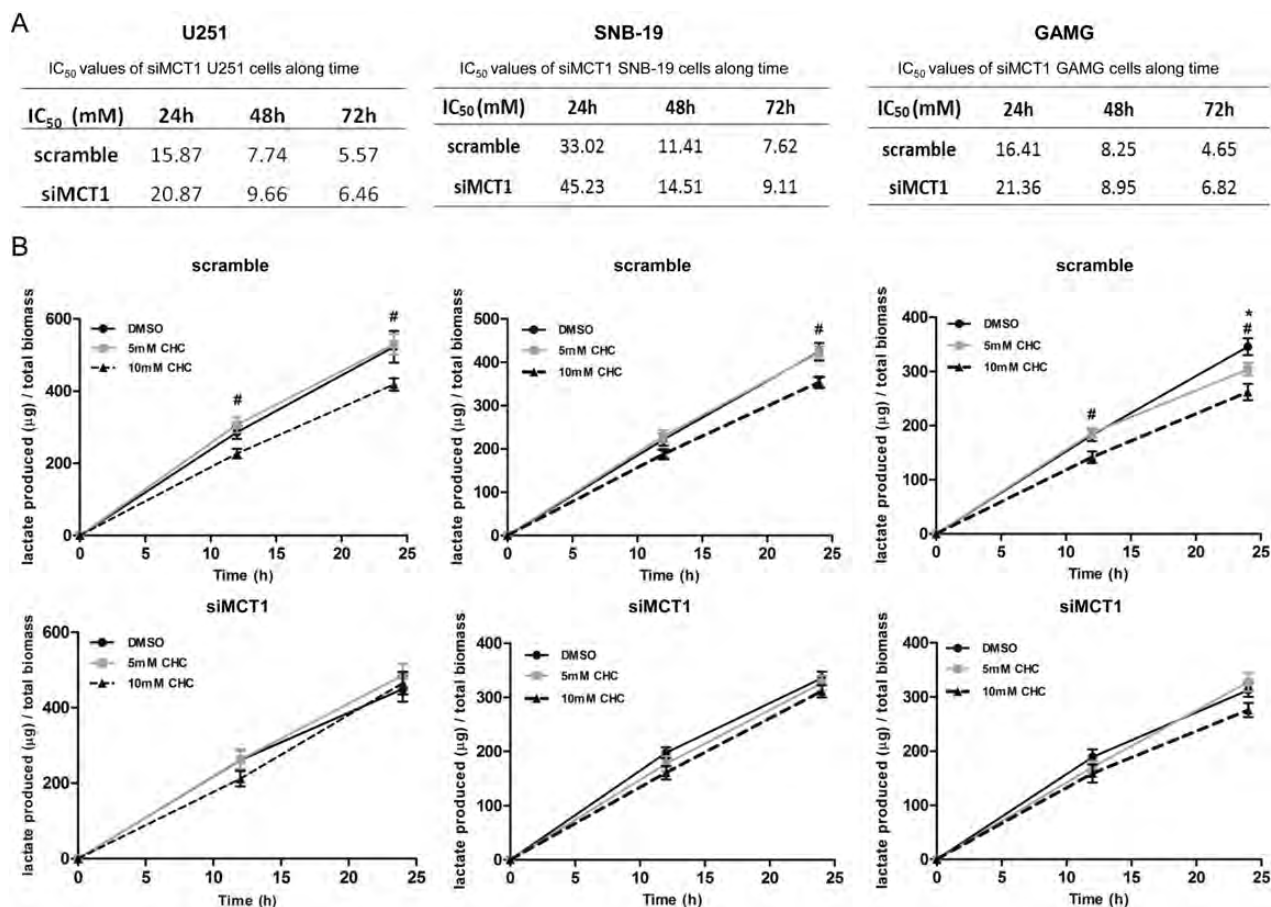


Fig. 7. Effect of MCT1 downregulation on the sensitivity to CHC. (A) IC<sub>50</sub> values for scramble and siMCT1 cells were determined over time by total cell biomass. (B) Effect of CHC on lactate production in siMCT1 cells over time. \* $P \leq .05$ , 5 mM CHC compared with DMSO. # $P \leq .05$ , 10 mM CHC compared with DMSO. Results are expressed as the mean  $\pm$  SD of at least 3 independent experiments, each in triplicate.

accompanied by an increased ratio of lactate to pyruvate.<sup>39</sup> Thus, upregulation of MCTs likely plays an important role in glioma intracellular homeostasis and, thus, contributes to its high aggressiveness.

In the present study, we observed that MCT1 and MCT4 were upregulated in glioblastomas, compared with nonneoplastic brain tissues. Compared with diffuse astrocytomas, no significant differences were observed, possibly because of the small number of cases evaluated. Our results are in accordance with the study of Froberg et al.,<sup>30</sup> who showed that MCT1 was upregulated in glioblastoma tissues ( $n = 17$ ), compared with normal brain and low-grade astrocytomas ( $n = 14$ ). However, unlike our study, the authors did not describe the cellular localization of MCT1 expression, essential for the role of MCTs in intracellular homeostasis. MCT4 expression has not previously been looked at in brain tumors. MCT4 is increased in glioblastomas, compared with nonneoplastic brain tissue, and in a high number of glioblastomas, MCT4 was present in the cytoplasm (43.7% [31/71]), in opposition to MCT1. The high expression of MCT4 in the cytoplasm may reflect its role in lactate-pyruvate transport in other

intracellular organelles.<sup>40,41</sup> Thus, our results suggest that MCT1 would be preferentially involved in lactate efflux, as an adaptation to the glycolytic phenotype in glioblastomas. In addition to being an MCT1 and MCT4 chaperone, CD147 is described as a key element in oncogenesis<sup>42</sup> and is upregulated in many human tumors. In the present study, CD147 expression increased with malignancy, with a significant increase from nonneoplastic tissue to diffuse astrocytomas and high-grade gliomas. Our results are in accordance with the study of Sameshima et al., in which it was shown that CD147 was highly expressed in glioblastomas ( $n = 9$ ) but not in low-grade gliomas ( $n = 9$ ) or nonneoplastic brain tissue ( $n = 12$ ).<sup>43</sup> In addition, our results showed an association of both MCT1 and MCT4 with CD147 plasma membrane expression, supporting the role of CD147 as chaperone for both MCT isoforms in gliomas.

We observed that MCT1, MCT4, and CD147 are expressed in the glioma cell lines studied, however, with different expression levels and cellular localization and with a pattern similar to glioblastoma tissues. To understand the biological role of MCTs, we performed in vitro

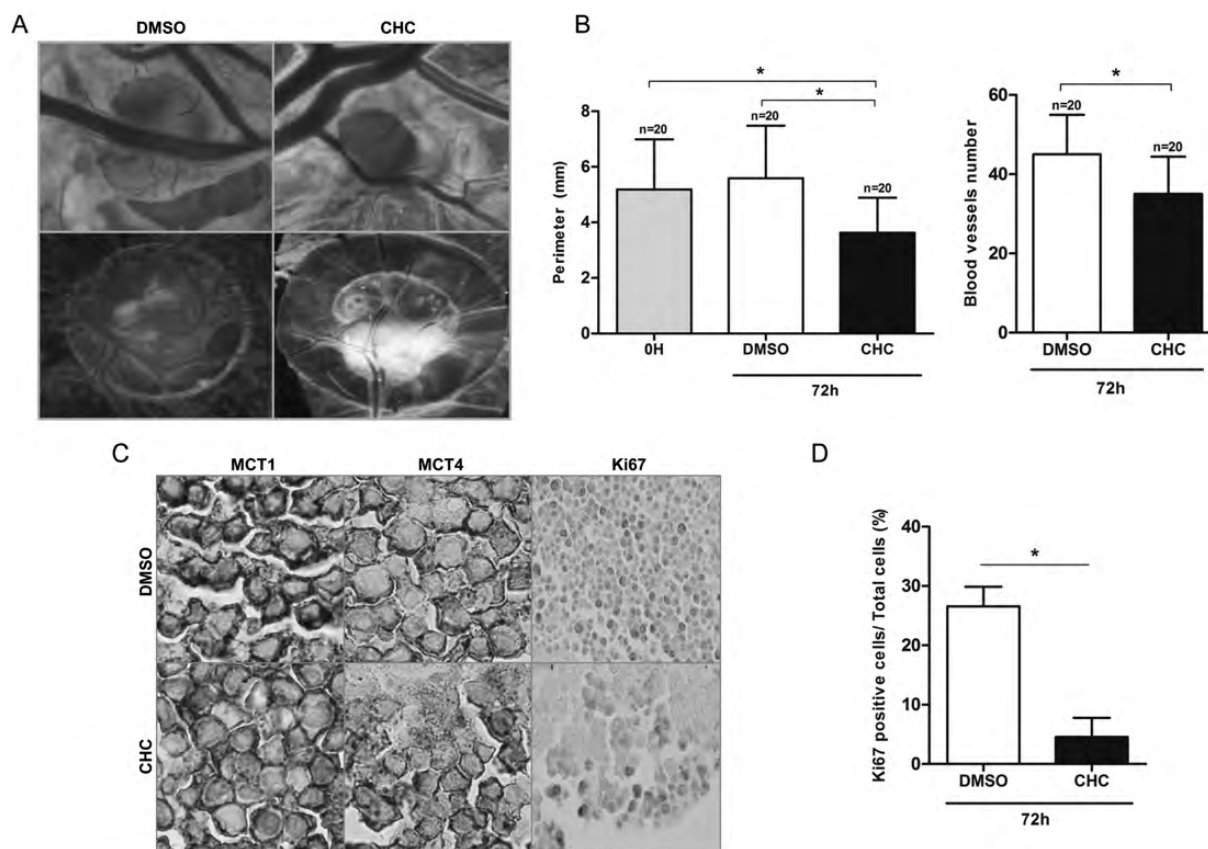


Fig. 8. In vivo effect of CHC in U251 glioma cell growth. (A) Representative pictures ( $16\times$  [up] and  $12.5\times$  [down] magnifications) of CAM assay after 7 days of tumor growth ex ovo. Representative pictures of CHC effect on the perimeter (up) and in vascularization (down) of tumors. (B) Tumor growth was measured in vivo, and blood vessels around the tumors were counted ex ovo, as described in the Materials and Methods section. A significant decrease in the perimeter (mm) of the tumors treated with 5 mM CHC (left graph) (control group  $n = 20$ ; CHC group  $n = 20$ ) was observed. CHC decreased the number of vessels around the tumors, compared with the control group (right graph) (control group  $n = 20$ ; CHC group  $n = 20$ ). (C) Representative pictures ( $400\times$  magnification) of immunohistochemical analysis of MCT1, MCT4, and Ki67 expression in tumors of control compared with CHC group. CHC did not induce an effect in the cellular localization and expression of MCT1 and MCT4. In Ki67 immunoreaction, we observed a decrease in the number of U251-stained cells in the CHC group, compared with control group. (D) Percentage of Ki67 positive cells. CHC group had a lower number of Ki67 positive cells (5%,  $n = 5$ ), compared with the control group (25%,  $n = 5$ ); data are the mean  $\pm$  SD.  $*P \leq .05$ .

and in vivo assays using CHC, a classical MCT inhibitor. Despite the availability of other MCT inhibitors, such as 4,4'-diisothiocyanostilbene-2,2'-disulphonate (DIDS),<sup>44</sup> quercetin,<sup>45</sup> and lonidamine (LND),<sup>46</sup> CHC is the best described in the literature as having MCTs, namely MCT1, as a primary target,<sup>47</sup> which of importance, shows no toxicity in in vivo models.<sup>35,36</sup> Nevertheless, CHC and all the other compounds may have other targets. It is described that CHC inhibits the chloride-bicarbonate exchanger AE1 with lower affinity.<sup>12</sup> DIDS inhibits AE1 more powerfully than MCTs,<sup>12</sup> and quercetin has various intracellular targets, inhibiting signaling molecules involved in cell survival and proliferation.<sup>48</sup> LND inhibits lactate transportation,<sup>46,49</sup> decreasing intracellular pH;<sup>50</sup> however, it is well described that the LND primary target is the hexokinase II (HKII) enzyme activity.<sup>51,52</sup>

We verified that most glioma cell lines were sensitive to CHC, with the exception of SW1088 and SW1783

cells, which showed lower sensitivity. The effect of CHC on U251 and SW1088 total cell biomass appears to be related to lactate transport activity. Accordingly, U251 cells presented higher levels of MCT1 and CD147 at the plasma membrane than did SW1088, and consequently, CHC decreased glucose consumption and lactate production in U251, but not in SW1088 cells. A decrease in glucose consumption is an expected result, because the blockage of lactate efflux likely leads to glycolysis arrest. In the sensitive U251 cells, CHC was able to inhibit cell proliferation and induce cell death, having a cytotoxic effect; however, in the less sensitive SW1088 cells, CHC only inhibited cell proliferation but did not induce cell death, having only a cytostatic effect. We verify that MCT location was in agreement with the CHC effect on cell proliferation and/or cell death. Our findings support the dependence of CHC sensitivity on MCT plasma membrane expression. Results obtained by Mathupala et al. showed that

inhibition of MCTs by siRNA<sup>26</sup> and CHC<sup>27</sup> reduced cell viability and lactate efflux and promoted cell death in U87-MG cells; however, they did not associate these results with MCT cellular localization. MCT plasma membrane expression is essential for lactate efflux, contributing to the maintenance of the high glycolytic rates and to acidic microenvironment, important features in tumor invasive phenotype.<sup>6</sup> Thus, assessment of plasma membrane expression becomes crucial to explain the effect of CHC. Despite being described as an inhibitor of pyruvate transportation into the mitochondria,<sup>47</sup> recent studies indicate that CHC does not enter the cell,<sup>27,36</sup> because its inhibitory effect is dependent on interactions with membrane proteins accessible from the outside of the cell. It is known that CHC can inhibit different MCT isoforms;<sup>11</sup> however, they have different sensitivities. In this context, in addition to MCT1, CHC could also inhibit MCT4 activity; however, the latter should happen at much higher concentrations, because MCT4 has much lower affinity for CHC ( $K_i$  values are 5–10 times higher than for MCT1; 50–100 mM). Because we used concentrations of 0.6–12 mM CHC, it can be assumed that CHC effect is mediated by MCT1 inhibition.

CHC inhibited the migration and invasion capacity of the glycolytic U251 but not the less glycolytic SW1088 cells, suggesting that the glycolytic phenotype and MCT expression profile have an important role in the migration and invasive capacity of glioma cells, putatively through lactate efflux and consequent contribution to acidic microenvironment. Our results are in accordance with the recent published studies, which demonstrate that classical MCT inhibitors and knockdown of MCT1 and MCT4 reduced the migration and invasion capacity of breast, lung, and glioma cells.<sup>36,53,54</sup> Although the recent study published by Mathupala et al.<sup>36</sup> reported that CHC decreases the invasive capacity of glioma cells, the authors did not characterize MCT isoform expression and cellular location in glioma cells, which would be essential to show that the effect of CHC is mediated by lactate efflux inhibition through MCTs. Thus, according to the different MCT expression between both cell lines in study, our results suggest that MCT1 may have a crucial role in the highly invasive capacity of glioma cells, along with lactate<sup>55</sup> in the tumor microenvironment.

Overall, our results suggest that the effect of CHC on lactate transportation activity, namely lactate efflux, and consequently, proliferation, cell death, migration, and invasion activity may be mediated through MCT1 inhibition. It is known that MCTs are expressed in several human organs,<sup>13</sup> and therefore, some adverse effects are expected because of inhibition of lactate transport activity by CHC. However, Sonveaux et al.<sup>35</sup> and Colen et al.<sup>36</sup> demonstrated that CHC did not show apparent toxicity in the animal models used. Moreover, it was demonstrated that CHC effects in the normal brain tissue are minimal and do not have a significant impact in the neuron-astrocyte lactate shuttle.<sup>36</sup>

In addition, we showed that the use of CHC in combination with TMZ potentiated the effect of TMZ on glioma cell growth. These results suggest that CHC,

through lactate transport inhibition and consequent glycolytic flux arrest, makes glioma cells more sensitive to standard therapy. Thus, CHC becomes a promising drug for adjuvant therapy of patients with glioblastomas, sensitizing glioma cells to standard therapy, anticipating little impact on the integrity and viability of normal brain. The effect of CHC as adjuvant in glioma therapy was also demonstrated by Mathupala et al.,<sup>27</sup> who reported that U87-MG cells were more sensitive to radiotherapy with CHC pretreatment. Thus, our results for combination of CHC with standard therapy highlighted the importance to target glioma glycolytic metabolism, namely MCT activity; this will decrease lactate concentrations in the tumor microenvironment and, consequently, decrease the migration and invasive capacity of glioblastomas, which is also associated with resistance to standard therapy. TMZ has been described to have a pro-autophagic<sup>56</sup> and late apoptotic effect,<sup>57</sup> contributing also to an anti-angiogenic activity of gliomas when combined with bevacizumab.<sup>58</sup> These studies showed that the effect of TMZ in vivo was higher than in vitro, when the respective  $IC_{50}$  values were compared. Thus, the in vitro effect of TMZ could be masked by the cell culture conditions, and it might be important to test the relevance of CHC and TMZ combination in vivo. However, our study showed for the first time that CHC potentiates the action of TMZ, with a synergistic effect.

To clarify the role of MCT1 inhibition as the mechanism of CHC action, we downregulated MCT1 in U251, SNB-19, and GAMG glioma cell lines, which exhibited the highest MCT1 plasma membrane expression together with higher sensitivity to CHC. Downregulation of MCT1 led to a decrease in cell growth, proliferation, and migration, likely because of the observed decrease in lactate production. This indicates that MCT1 has an important role in glioma proliferation and progression. Downregulation of MCT1 expression in glioma cells conferred resistance to CHC, as observed by the increased  $IC_{50}$  values. Furthermore, treatment of siMCT1 cells with CHC did not change lactate production, providing further evidence for the specificity of CHC for MCT1, because MCT4 is still present at the plasma membrane in these cells, although at lower levels than in MCT1. Of interest, the decrease in CD147 expression after MCT1 downregulation that was observed in U251 and SNB-19 cells was not detected in GAMG cells. This fact could be explained by the higher MCT4 membrane expression in GAMG cells, which could have allowed the maintenance of CD147 expression. These observations are in agreement with the interdependence of MCT1/4 and CD147 described in the literature.<sup>54</sup>

Overall, inhibition of MCT1 expression was similar to inhibition of MCT1 activity, providing evidence for CHC-inhibition of MCT1 as the mechanism of selective toxicity observed in glioblastoma cells.

Furthermore, through in vivo studies, we observed a significant decrease in the size of U251 tumors formed in the CAM, validating the antitumoral activity of CHC against glioma cells. This was further confirmed

by a decrease in proliferation of glioma cells with CHC treatment. These observations support the *in vitro* results, where it was reported that CHC decreases cell growth and promotes cell death. Although the CAM assay is not a full *in vivo* assay, it has been used as a rapid, economic, and reliable approach for drug screening, as demonstrated by other groups.<sup>37,59–61</sup> In addition, we observed that CHC had an inhibitory effect in the CAM angiogenesis, demonstrated by a significant decrease in the vascularization associated with the formed tumors, which we showed was not attributable to direct effect of CHC on chicken endothelial cells. It is described that lactate increases VEGF production, the major angiogenic factor in the microenvironment,<sup>62</sup> and we observed that CHC decreased lactate production in U251 cells. Therefore, we hypothesized that treatment with CHC decreased tumor size and number of blood vessels, likely because of impairment of tumor glycolytic metabolism and decrease in VEGF production mediated by the decrease in microenvironment lactate concentrations.

In summary, in the present study, we demonstrated that MCT1 and MCT4, along with their chaperone CD147, are upregulated at the plasma membrane in glioblastomas. In addition, using *in vitro* and *in vivo* glioblastoma models, we demonstrated the effectiveness

of inhibiting the activity and expression of MCT1, particularly in more glycolytic cells. Of importance, a synergistic effect between CHC and TMZ was observed. Thus, the use of MCT1 inhibitors and probably other metabolic-targeting drugs should be explored as a novel strategy for glioblastoma treatment.

## Supplementary Material

Supplementary material is available at *Neuro-Oncology Journal* online (<http://neuro-oncology.oxfordjournals.org/>).

*Conflict of interest statement.* None declared.

## Funding

This work was supported by the Life and Health Sciences Research Institute, University of Minho, Portugal, and Fundação para a Ciência e Tecnologia (SFRH/BI/33503/2008 to V.M.G., SFRH/BPD/69479/2010 to C. P., and SFRH/BD/36463/2007 to O. M.).

## References

- Louis DN, Ohgaki H, Wiestler OD, et al. The 2007 WHO classification of tumours of the central nervous system. *Acta Neuropathol.* 2007;114(2):97–109.
- Stupp R, Hegi ME, Mason WP, et al. Effects of radiotherapy with concomitant and adjuvant temozolomide versus radiotherapy alone on survival in glioblastoma in a randomised phase III study: 5-year analysis of the EORTC-NCIC trial. *Lancet Oncol.* 2009;10(5):459–466.
- Dang CV, Semenza GL. Oncogenic alterations of metabolism. *Trends Biochem Sci.* 1999;24(2):68–72.
- Hanahan D, Weinberg RA. Hallmarks of cancer: the next generation. *Cell.* 2011;144(5):646–674.
- Gatenby RA, Gillies RJ. Why do cancers have high aerobic glycolysis? *Nat Rev Cancer.* 2004;4(11):891–899.
- Kroemer G, Pouyssegur J. Tumor cell metabolism: cancer's Achilles' heel. *Cancer Cell.* 2008;13(6):472–482.
- Vander Heiden MG, Cantley LC, Thompson CB. Understanding the Warburg effect: the metabolic requirements of cell proliferation. *Science.* 2009;324(5930):1029–1033.
- Gillies RJ, Robey I, Gatenby RA. Causes and consequences of increased glucose metabolism of cancers. *J Nucl Med.* 2008;49(suppl 2):24S–42S.
- Izumi H, Torigoe T, Ishiguchi H, et al. Cellular pH regulators: potentially promising molecular targets for cancer chemotherapy. *Cancer Treat Rev.* 2003;29(6):541–549.
- Halestrap AP, Price NT. The proton-linked monocarboxylate transporter (MCT) family: structure, function and regulation. *Biochem J.* 1999;343(pt 2):281–299.
- Enerson BE, Drewes LR. Molecular features, regulation, and function of monocarboxylate transporters: implications for drug delivery. *J Pharm Sci.* 2003;92(8):1531–1544.
- Halestrap AP, Meredith D. The SLC16 gene family—from monocarboxylate transporters (MCTs) to aromatic amino acid transporters and beyond. *Pflugers Arch.* 2004;447(5):619–628.
- Merezinskaya N, Fishbein WN. Monocarboxylate transporters: past, present, and future. *Histol Histopathol.* 2009;24(2):243–264.
- Pierre K, Pellerin L. Monocarboxylate transporters in the central nervous system: distribution, regulation and function. *J Neurochem.* 2005;94(1):1–14.
- Pellerin L, Bergersen LH, Halestrap AP, Pierre K. Cellular and subcellular distribution of monocarboxylate transporters in cultured brain cells and in the adult brain. *J Neurosci Res.* 2005;79(1–2):55–64.
- Kennedy KM, Dewhirst MW. Tumor metabolism of lactate: the influence and therapeutic potential for MCT and CD147 regulation. *Future Oncol.* 2010;6(1):127–148.
- Pellerin L. Lactate as a pivotal element in neuron-glia metabolic cooperation. *Neurochem Int.* 2003;43(4–5):331–338.
- Kirk P, Wilson MC, Hedde C, Brown MH, Barclay AN, Halestrap AP. CD147 is tightly associated with lactate transporters MCT1 and MCT4 and facilitates their cell surface expression. *EMBO J.* 2000;19(15):3896–3904.
- Wilson MC, Meredith D, Fox JE, Manoharan C, Davies AJ, Halestrap AP. Basigin (CD147) is the target for organomercurial inhibition of monocarboxylate transporter isoforms 1 and 4: the ancillary protein for the insensitive MCT2 is EMBIGIN (gp70). *J Biol Chem.* 2005;280(29):27213–27221.
- Walenta S, Wetterling M, Lehrke M, et al. High lactate levels predict likelihood of metastases, tumor recurrence, and restricted patient survival in human cervical cancers. *Cancer Res.* 2000;60(4):916–921.

21. Pinheiro C, Albergaria A, Paredes J, et al. Monocarboxylate transporter 1 is up-regulated in basal-like breast carcinoma. *Histopathology*. 2010;56(7):860–867.
22. Pinheiro C, Longatto-Filho A, Scapulatempo C, et al. Increased expression of monocarboxylate transporters 1, 2, and 4 in colorectal carcinomas. *Virchows Arch*. 2008;452(2):139–146.
23. Pinheiro C, Longatto-Filho A, Ferreira L, et al. Increasing expression of monocarboxylate transporters 1 and 4 along progression to invasive cervical carcinoma. *Int J Gynecol Pathol*. 2008;27(4):568–574.
24. Koukourakis MI, Giatromanolaki A, Bougioukas G, Sivridis E. Lung cancer: a comparative study of metabolism related protein expression in cancer cells and tumor associated stroma. *Cancer Biol Ther*. 2007;6(9):1476–1479.
25. Pinheiro C, Longatto-Filho A, Simoes K, et al. The prognostic value of CD147/EMMPRIN is associated with monocarboxylate transporter 1 co-expression in gastric cancer. *Eur J Cancer*. 2009;45(13):2418–2424.
26. Mathupala SP, Parajuli P, Sloan AE. Silencing of monocarboxylate transporters via small interfering ribonucleic acid inhibits glycolysis and induces cell death in malignant glioma: an in vitro study. *Neurosurgery*. 2004;55(6):1410–1419; discussion 1419.
27. Colen CB, Seraji-Bozorgzad N, Marples B, Galloway MP, Sloan AE, Mathupala SP. Metabolic remodeling of malignant gliomas for enhanced sensitization during radiotherapy: an in vitro study. *Neurosurgery*. 2006;59(6):1313–1323; discussion 1323–1314.
28. Fang J, Quinones QJ, Holman TL, et al. The H<sup>+</sup>-linked monocarboxylate transporter (MCT1/SLC16A1): a potential therapeutic target for high-risk neuroblastoma. *Mol Pharmacol*. 2006;70(6):2108–2115.
29. Li KK, Pang JC, Ching AK, et al. miR-124 is frequently down-regulated in medulloblastoma and is a negative regulator of SLC16A1. *Hum Pathol*. 2009;40(9):1234–1243.
30. Froberg MK, Gerhart DZ, Enerson BE, et al. Expression of monocarboxylate transporter MCT1 in normal and neoplastic human CNS tissues. *Neuroreport*. 2001;12(4):761–765.
31. Pinheiro C, Longatto-Filho A, Pereira SM, et al. Monocarboxylate transporters 1 and 4 are associated with CD147 in cervical carcinoma. *Dis Markers*. 2009;26(3):97–103.
32. Martinho O, Granja S, Jaraquemada T, et al. Downregulation of RKIP is associated with poor outcome and malignant progression in gliomas. *PLoS One*. 2012;7(1):e30769.
33. Chou TC. Theoretical basis, experimental design, and computerized simulation of synergism and antagonism in drug combination studies. *Pharmacol Rev*. 2006;58(3):621–681.
34. Moniz S, Matinho O, Pinto F, et al. Loss of WNK2 expression by promoter gene methylation occurs in adult gliomas and triggers Rac1-mediated tumour cell invasiveness. [published online ahead of print October 22, 2012]. *Hum Mol Genet*. 2012. doi:10.1093/hmg/dd5405.
35. Sonveaux P, Vegran F, Schroeder T, et al. Targeting lactate-fueled respiration selectively kills hypoxic tumor cells in mice. *J Clin Invest*. 2008;118(12):3930–3942.
36. Colen CB, Shen Y, Ghoddoussi F, et al. Metabolic targeting of lactate efflux by malignant glioma inhibits invasiveness and induces necrosis: an in vivo study. *Neoplasia*. 2011;13(7):620–632.
37. Hagedorn M, Javerzat S, Gilges D, et al. Accessing key steps of human tumor progression in vivo by using an avian embryo model. *Proc Natl Acad Sci U S A*. 2005;102(5):1643–1648.
38. Oudard S, Arvelo F, Miccoli L, et al. High glycolysis in gliomas despite low hexokinase transcription and activity correlated to chromosome 10 loss. *Br J Cancer*. 1996;74(6):839–845.
39. Tabatabaei P, Bergstrom P, Henriksson R, Bergenheim AT. Glucose metabolites, glutamate and glycerol in malignant glioma tumours during radiotherapy. *J Neurooncol*. 2008;90(1):35–39.
40. Dubouchaud H, Butterfield GE, Wolfel EE, Bergman BC, Brooks GA. Endurance training, expression, and physiology of LDH, MCT1, and MCT4 in human skeletal muscle. *Am J Physiol Endocrinol Metab*. 2000;278(4):E571–E579.
41. Benton CR, Campbell SE, Tonouchi M, Hatta H, Bonen A. Monocarboxylate transporters in subsarcolemmal and intermyofibrillar mitochondria. *Biochem Biophys Res Commun*. 2004;323(1):249–253.
42. Nabeshima K, Iwasaki H, Koga K, Hojo H, Suzumiya J, Kikuchi M. Emmprin (basigin/CD147): matrix metalloproteinase modulator and multifunctional cell recognition molecule that plays a critical role in cancer progression. *Pathol Int*. 2006;56(7):359–367.
43. Sameshima T, Nabeshima K, Toole BP, et al. Expression of emmprin (CD147), a cell surface inducer of matrix metalloproteinases, in normal human brain and gliomas. *Int J Cancer*. 2000;88(1):21–27.
44. Poole RC, Halestrap AP. Reversible and irreversible inhibition, by stilbenedisulphonates, of lactate transport into rat erythrocytes. Identification of some new high-affinity inhibitors. *Biochem J*. 1991;275(pt 2):307–312.
45. Belt JA, Thomas JA, Buchsbaum RN, Racker E. Inhibition of lactate transport and glycolysis in Ehrlich ascites tumor cells by bioflavonoids. *Biochemistry*. 1979;18(16):3506–3511.
46. Floridi A, Paggi MG, D'Atri S, et al. Effect of lonidamine on the energy metabolism of Ehrlich ascites tumor cells. *Cancer Res*. 1981;41(11 pt 1):4661–4666.
47. Halestrap AP, Denton RM. Specific inhibition of pyruvate transport in rat liver mitochondria and human erythrocytes by alpha-cyano-4-hydroxycinnamate. *Biochem J*. 1974;138(2):313–316.
48. Senthilkumar K, Arunkumar R, Elumalai P, et al. Quercetin inhibits invasion, migration and signalling molecules involved in cell survival and proliferation of prostate cancer cell line (PC-3). *Cell Biochem Funct*. 2011;29(2):87–95.
49. Ben-Yoseph O, Lyons JC, Song CW, Ross BD. Mechanism of action of lonidamine in the 9L brain tumor model involves inhibition of lactate efflux and intracellular acidification. *J Neurooncol*. 1998;36(2):149–157.
50. Zhou R, Bansal N, Leeper DB, Pickup S, Glickson JD. Enhancement of hyperglycemia-induced acidification of human melanoma xenografts with inhibitors of respiration and ion transport. *Acad Radiol*. 2001;8(7):571–582.
51. Mathupala SP, Ko YH, Pedersen PL. Hexokinase II: cancer's double-edged sword acting as both facilitator and gatekeeper of malignancy when bound to mitochondria. *Oncogene*. 2006;25(34):4777–4786.
52. Pelicano H, Martin DS, Xu RH, Huang P. Glycolysis inhibition for anticancer treatment. *Oncogene*. 2006;25(34):4633–4646.
53. Izumi H, Takahashi M, Uramoto H, et al. Monocarboxylate transporters 1 and 4 are involved in the invasion activity of human lung cancer cells. *Cancer Sci*. 2011;102(5):1007–1013.
54. Gallagher SM, Castorino JJ, Wang D, Philp NJ. Monocarboxylate transporter 4 regulates maturation and trafficking of CD147 to the plasma membrane in the metastatic breast cancer cell line MDA-MB-231. *Cancer Res*. 2007;67(9):4182–4189.



55. Baumann F, Leukel P, Doerfelt A, et al. Lactate promotes glioma migration by TGF-beta2-dependent regulation of matrix metalloproteinase-2. *Neuro Oncol.* 2009;11(4):368–380.
56. Kanzawa T, Germano IM, Komata T, Ito H, Kondo Y, Kondo S. Role of autophagy in temozolomide-induced cytotoxicity for malignant glioma cells. *Cell Death Differ.* 2004;11(4):448–457.
57. Roos WP, Batista LF, Naumann SC, et al. Apoptosis in malignant glioma cells triggered by the temozolomide-induced DNA lesion O6-methylguanine. *Oncogene.* 2007;26(2):186–197.
58. Mathieu V, De Neve N, Le Mercier M, et al. Combining bevacizumab with temozolomide increases the antitumor efficacy of temozolomide in a human glioblastoma orthotopic xenograft model. *Neoplasia.* 2008;10(12):1383–1392.
59. Sihm G, Walter T, Klein JC, et al. Anti-angiogenic properties of myo-inositol trispyrophosphate in ovo and growth reduction of implanted glioma. *FEBS Lett.* 2007;581(5):962–966.
60. Saidi A, Hagedorn M, Allain N, et al. Combined targeting of interleukin-6 and vascular endothelial growth factor potently inhibits glioma growth and invasiveness. *Int J Cancer.* 2009;125(5):1054–1064.
61. Brignole C, Marimpietri D, Pastorino F, et al. Effect of bortezomib on human neuroblastoma cell growth, apoptosis, and angiogenesis. *J Natl Cancer Inst.* 2006;98(16):1142–1157.
62. Kumar VB, Viji RI, Kiran MS, Sudhakaran PR. Endothelial cell response to lactate: implication of PAR modification of VEGF. *J Cell Physiol.* 2007;211(2):477–485.